J. Membrane Biol. 212, 147–161 (2006)
DOI: 10.1007/s00232-006-0044-z

The Journal of
Membrane
Biology

Role of Sustained Overexpression of Central Nervous System IGF-I in the Age-Dependent Decline of Mouse Excitation-Contraction Coupling

Ramón Jiménez Moreno[1], María Laura Messi[1], Zhenlin Zheng[1], Zhong-Min Wang[1], Ping Ye[2], Joseph A. D'Ercole[2], Osvaldo Delbono[1,3,4]

[1]Department of Physiology and Pharmacology, Wake Forest University School of Medicine, Winston-Salem, NC 27157, USA
[2]Department of Pediatrics, University of North Carolina at Chapel Hill, Chapel Hill, NC 27599, USA
[3]Department of Internal Medicine, Section on Gerontology, Wake Forest University School of Medicine, Winston-Salem, NC 27157, USA
[4]Neuroscience Program, Wake Forest University School of Medicine, Winston-Salem, NC 27157, USA

Received: 16 June 2006/Revised: 18 September 2006

Abstract. We investigated the effects of exclusive and sustained transgenic overexpression of insulin-like growth factor (IGF)-I in the central nervous system (CNS) on the age-dependent decline in muscle strength, excitation-contraction coupling, muscle innervation and neuromuscular junction postterminal architecture. We found that (1) transgenic IGF-I overexpression in the CNS does not modify the decline in extensor digitorum longus (EDL) and soleus muscle weight with aging and (2) strength significantly decreases in transgenic (Tg) compared to wild-type mice. The latter finding is consistent with (3) the decreased absolute and specific force measured in the EDL muscle *in vitro* and (4) the decreased charge movement and peak intracellular Ca^{2+} mobilization in individual muscle fibers from old IGF-I Tg mice compared to young wild-type mice, which also is associated with (5) decreased dihydropyridine receptor α_1-subunit expression in old compared to young IGF-I Tg mice. (6) Tg IGF-I prevents a change in muscle fiber type that is associated with (7) improved muscle innervation and postterminal neuromuscular structure. (8) IGF-I is expressed extensively across the spinal cord gray matter and the lateral motor column. Our results raise questions about the timing and cell location of CNS IGF-I overexpression necessary to prevent or to ameliorate age-dependent alterations in the structure and function of skeletal muscle.

Key words: Aging — Insulin-like growth factor-I — Skeletal muscle — Calcium channel

Introduction

Age-related decline in the neuromuscular system is a recognized cause of impaired physical performance and loss of independence in the elderly. The decline in muscle strength recorded in humans and rodents is due to declines in both muscle mass (Lexell, 1995) and muscle fiber-specific force (Brooks & Faulkner, 1988; Gonzalez, Messi & Delbono, 2000). Age-related motor unit remodeling, characterized by denervation and reinnervation (Larsson & Ansved, 1995; Kadhiresan, Hassett & Faulkner, 1996), accounts for the loss in muscle mass (Lexell, 1995), the shift in fiber type composition (Einsiedel & Luff, 1992; Lexell, 1995) and the decline in muscle-specific force (Delbono, 2003; Payne & Delbono, 2004).

Insulin-like growth factor-I (IGF-I) plays a central role in skeletal muscle and neuron structure and function. It induces proliferation, differentiation and repair in muscle cells (Florini, Ewton & Coolican, 1996; Mourkioti & Rosenthal, 2005), while it is a potent trophic factor for motor neurons (Caroni & Grandes, 1990; Li et al., 1994). IGF-I also inhibits neural cell apoptosis during postnatal life (Popken et al., 2004), and its administration prevents motor neuron cell death and enhances reinnervation after nerve injury (Kanje et al., 1989; Li et al., 1999). IGF-I from skeletal muscle exerts a target-derived trophic effect on survival of embryonic motor neurons (Neff et al., 1993) and muscle innervation in aged animals (Messi & Delbono, 2003); consequently, its overexpression exclusively in skeletal muscle enhances motor

Ramón Jiménez Moreno and María Laura Messi contributed equally to this work.

Correspondence to: Osvaldo Delbono; email: odelbono@wfubmc.edu

neuron reinnervation after nerve injury (Rabinovsky et al., 2003) and prevents, to a certain extent, motor neuron death in the degenerative disease amyotrophic lateral sclerosis (Dobrowolny et al., 2005).

Overexpression of IGF-I in muscle produces muscle hypertrophy in transgenic (Tg) mice (Coleman et al., 1995; Florini et al., 1996; Musaro et al., 2001). IGF-I also increases the contribution of bone marrow-derived cells to regenerating adult skeletal muscle (Sacco et al., 2005). Its overexpression in skeletal muscle prevents age-related loss in muscle mass (Barton-Davis et al., 1998; Musaro et al., 2001) and excitation-contraction uncoupling (Renganathan, Messi & Delbono, 1998; Wang, Messi & Delbono, 2002) and maintains skeletal muscle fiber-specific force (Renganathan et al., 1998; González et al., 2003) in aged mice. These findings may be due to its direct effect on skeletal muscle dihydropyridine receptor (DHPR) transcription (Zheng, Wang & Delbono, 2002), which is mediated by Ca^{2+} calmodulin kinase and calcineurin activation (Zheng, Wang & Delbono, 2004), or to its target-derived trophic effects on motor neurons in aged mice via maintenance of muscle fiber innervation, which have been established for mature and senescent mice (Messi & Delbono, 2003).

We recently demonstrated that targeted human IGF-I (hIGF-I) delivery to motor neurons through injection of an hIGF-I/tetanus toxin fragment C fusion protein into hindlimb skeletal muscles prevents specific force decline in aging mouse muscle (Payne et al., 2005). However, we do not know the mechanism(s) by which IGF-I overexpression in spinal cord motor neurons prevents force decline with aging. The present work examined whether sustained overexpression of IGF-I exclusively in the central nervous system (CNS) can prevent decline in muscle absolute force by acting on muscle mass and the mechanism by which IGF-I averts the age-dependent decrease in muscle-specific force.

Methods

IGF-I Tg Mice

Previously described IGF-I Tg mice, termed IGF-2/1 Tg mice (Ye et al., 1996), were used for the study. These mice overexpress hIGF-I exclusively in the CNS under the control of a 5.7—kb DNA fragment of the 5′ mouse IGF-II genomic regulatory region (Dai et al., 1992; Ye et al., 1996). They are routinely bred as heterozygotes with C57BL/6 mice and identified by polymerase chain reaction of tail genomic DNA. Non-Tg littermate C57BL/6 mice were used as controls. Mice were maintained with 12:12 h (light:dark) cycles at 22°C. An aging colony was housed in a pathogen-free facility of the Wake Forest University School of Medicine (WFUSM) Animal Resources Program. Mice exhibiting gross external or internal pathology at macroscopic inspection were not included in the study. All procedures were approved by the WFUSM Animal Care and Use Committee.

Muscle Contraction

Young (3–5 months) and old (24–27 months) IGF-2/1 Tg mice and C57BL/6 control littermates were used for contraction experiments. Mice were killed by cervical dislocation. Extensor digitorum longus (EDL) and soleus muscle contraction followed published procedures (González et al., 2003). Force was recorded using a 407A force transducer (Aurora, Ontario, Canada) or a Harvard (Holliston, MA) 60–2996 model. Muscle cross-sectional area (CSA) was calculated as described (Segal & Faulkner, 1985). Specific force (in kPa) was calculated as maximum tetanic force (kN)/CSA (m^2).

Neuromuscular Strength: Retention Time

Tg and wild-type mice were tested for their ability to remain hanging from a wire, following described procedures (Ogura, Aruga & Mikoshiba, 2001) with some modifications. They were tested three times per day over 6 consecutive days, and the average and best retention times were computed. The amount of time spent hanging was recorded and scored according to the following system: 0, fell off; 1, hung onto the bar with two forepaws; 2, in addition to 1, attempted to climb onto the bar; 3, hung onto the bar with two forepaws and one or both hindpaws; 4, hung onto the bar with all four paws with tail wrapped around the bar; 5, escaped to one of the supports (Ogura et al., 2001). Additionally, the same animals used for retention time were tested for muscle grip strength (Meyer et al., 1979). For these measurements, we used a grip strength meter provided with a Chatillon Digital Force Gauge DFIS 2 (Columbus Instruments, Columbus, OH), and mice were followed for 6 days, given the reproducibility of the measurements.

Charge Movement Recordings

For charge movement and intracellular Ca^{2+} recordings in flexor digitorum brevis (FDB) muscle fibers, we followed published procedures (Wang, Messi & Delbono, 1999, 2002). For analysis of the charge's voltage dependence, data points were fitted to a Boltzmann equation:

$$Q_{on}=Q_{max}/[1+\exp(V_{1/2}Q-V\mathrm{m})/K] \quad (1)$$

where Q_{max} is the maximum charge, V_m is the membrane potential, $V_{1/2Q}$ is the charge movement at half-activation potential and K is the steepness of the curve.

Intracellular Ca^{2+} Recordings

For intracellular Ca^{2+} recordings, FDB fibers were loaded with 200 μM calcium-green (Invitrogen-Molecular Probes, Eugene, OR) via the patch pipette. The pipette solution was identical to that used for charge movement recordings, except the ethyleneglycoltetraacetic acid (EGTA) concentration was reduced to 0.2 mM. Ca^{2+} transients were elicited with 20-ms depolarizing pulses from the holding potential (−80 mV) to command potentials ranging from −40 to 30 mV.

For Ca^{2+} fluorescent recordings, the fibers were illuminated with a laser beam at 488 nm wavelength using a Bio-Rad (Thornwood, NY) Radiance 2100K−1 confocal scanning microscope and a 20X Fluar objective (Zeiss, Thornwood, NY). Emitted fluorescence was collected by the objective and directed to the head scanner, in open pinhole mode, through the emission filter at 525 nm wavelength before being collected by a photomultiplier tube and digitized. Hardware control, image acquisition and processing were performed with Lasersharp (Bio-Rad) run on a personal computer. For data analysis, several regions of interest were se-

lected for each cell, and maximum fluorescence deflection was used. For analysis of the voltage dependence of peak intracellular Ca^{2+} concentration, data points were fitted to the Boltzmann equation (equation 1).

For intracellular Ca^{2+} quantification, fluorescent signals were converted into Ca^{2+} concentration, following methods previously described (González et al., 2003) with some modifications. Briefly, we measured the K_d of calcium-green for Ca^{2+} *in vivo*, using FDB fibers acutely dissociated by the procedures described above. Single fibers were incubated with calcium-green AM (5 μM) and *N*-benzyl-*p*-toluenesulfonamide (50 μM; TRC, North York, Canada) for 30–40 min. After cell loading, the dye was washed out and the fiber exposed to different standard Ca^{2+} concentration solutions (0–100 μM), calculated according to published methods (Tsien & Pozzan, 1989). Under these conditions, basal fluorescence was recorded. Fibers were then permeabilized by applying 0.01% saponin to allow Ca^{2+} entry. No movement or morphological distortion was observed in any of the fibers. Each experimental point represents the mean of the recordings of at least four cells. The fluorescence at different pCa values was normalized to the maximum, and the mean values were fitted to the following equation: $y = 1/\{1 + (K_d/[Ca^{2+}])\}$. The K_d for calcium-green, measured in these conditions, was 27 μM, which is consistent with previous values reported by our laboratory (Wang, Messi & Delbono, 2000). Maximum fluorescence (F_{max}) was measured at the end of the experiment in each individual cell by applying a large depolarization (+60 m*V*) for 300 ms. F_{min}, the fluorescence at rest, was measured in a group of fibers ($n = 7$) equilibrated with 2 mM 1,2-bis(*o*-aminophenoxy)ethane-*N,N,N′,N′*-tetraacetic acid acetoxymethyl ester (BAPTA AM). Intracellular Ca^{2+} concentration was calculated using the following equation:

$$[Ca^{2+}]_i = K_d(F - F_{min})/(F_{max} - F) \quad (2)$$

where K_d is the dissociation constant and F is the peak fluorescence value recorded (Tsien & Pozzan, 1989). Ca^{2+} saturation was ruled out by the low affinity of the Ca^{2+} indicator (Wang et al., 2000).

Quantitative Determination of IGF-I Concentration

IGF-I concentration in serum, various regions of the CNS, skeletal muscle and peripheral organs was determined by radioimmunoassay associated with IGF-I binding protein blockade. The radioimmunoassay kit (Alpco Diagnostics, Windham, NH) uses a specific, high-affinity polyclonal antibody, whose cross-reactivity with IGF-II is $< 0.05\%$. The sensitivity of the assay is 0.02 ng/ml.

Myosin Heavy Chain Isoform Composition in EDL and Soleus Muscles

Myosin heavy chain (MHC) composition was determined by sodium dodecyl sulfate-polyacrylamide gel electrophoresis (SDS-PAGE), as described previously (Serrano et al., 1996) with some modifications (Messi & Delbono, 2003). Gels were silver-stained according to published protocols (Giulian, Moss & Greaser, 1983). As a reference for the four MHC isoforms (I, IIa, IIx, IIb), mouse diaphragm was used.

Motor Nerve Terminal and Cholinesterase Staining and Neuromuscular Junction Postterminal Staining

A combined stain for demonstrating motor nerve terminals and cholinesterase at the neuromuscular junctions was used (Pestronk & Drachman, 1978) with some modifications (Messi & Delbono, 2003). Postsynaptic acetylcholine receptor staining was performed as described (Messi & Delbono, 2003). The postterminal area was calculated in pixels by tracing the perimeter of individual, labeled regions on the digitized images and then converted into square micrometers.

Spinal Cord IGF-I Immunofluorescence

Mice were killed by cervical dislocation, and lumbar enlargements of spinal cords were collected after transcardiac perfusion of the mice with 4% paraformaldehyde in phosphate-buffered saline (PBS). Samples were stored in 4% paraformaldehyde in PBS overnight at 4°C, followed by storage in 20% sucrose in PBS for 36–48 h at 4°C. Spinal cords were then embedded in optimal cutting temperature (OCT) medium and frozen in liquid nitrogen. All samples were stored at −80°C until use.

For immunofluorescent detection of IGF-I in spinal cords, frozen samples were cut on a cryostat microtome cooled to −20°C (12 μm). They were blocked with 5% donkey serum and 0.02% Triton X-100 in PBS for 30 min. Spinal cord sections were incubated with mouse anti-IGF-I (Su et al., 1997) for 2 h at room temperature and then washed four times, 10 min each time, in PBS. Samples were then incubated with donkey antimouse immunoglobulin G conjugated with fluorescein isothiocyanate, diluted 1:100 in 2% donkey serum in PBS for 1 h at room temperature, and washed four times for 10 min in PBS. Spinal cord fluorescence was then imaged using an Axioskop 2 microscope and a charge-coupled device camera-based imaging system (see above).

DHPR α_1-Subunit Immunoblots

Microsome Preparation

Microsomes from mouse skeletal muscle were prepared as described (Knudson et al., 1989) with modifications. After protein concentration was measured by bicinchoninic acid protein assay, samples were mixed with double-strength sample buffer (Murray & Ohlendieck, 1997). All samples were kept at room temperature for 30 min, separated on 10% denaturing SDS-PAGE gels and transferred to polyvinylidene difluoride (PVDF) membranes.

Immunoblot

PVDF membranes with microsome preparations and immunoprecipitation were blocked by incubating the membranes with 5% milk/PBS for 30–60 min at room temperature. Membranes were then incubated with a mouse anti-DHPRα_1 antibody (kindly provided by Dr. Kevin P. Campbell, University of Iowa, Howard Hughes Medical Institute, Iowa City, IA) (Leung, Imagawa & Campbell, 1987) for 2 h at room temperature. The concentration of the DHPRα_1 antibody was 1:1,000 in 5% milk/1 x PBS. Finally, the membrane was incubated in enhanced chemiluminescence reagent (Amersham, Arlington Heights, IL) and visualized by X-ray film.

Data Analysis

Values are given as mean ± standard error of the mean (SEM) for the number of observations (n). Statistical analysis was performed using analysis of variance, followed by multiple comparisons (Student-Newman-Keuls test). The Mann-Whitney rank sum test was used for two-group comparisons when the data distribution was not normal. $P < 0.05$ was considered significant.

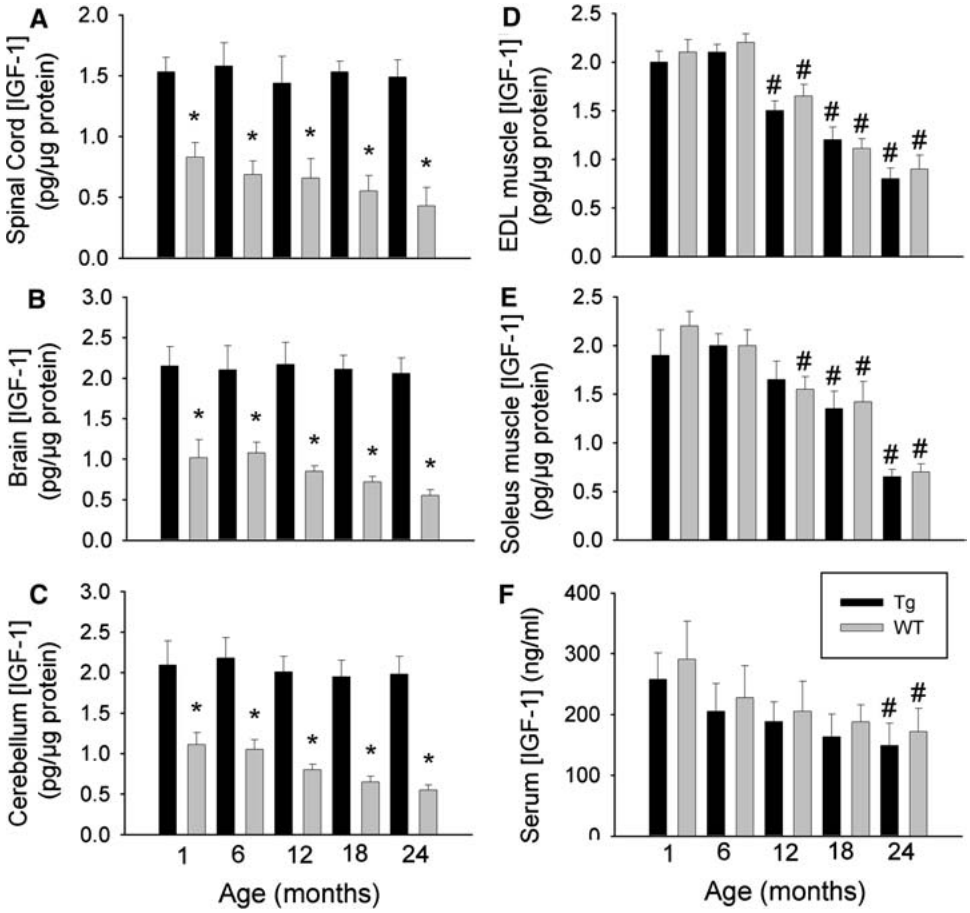

Fig. 1. IGF-I concentrations in regions of the CNS, skeletal muscle and serum. IGF-I concentrations in EDL and soleus muscle and serum from old (24 months) mice are significantly different from those recorded in young (1–6 months) mice ($P < 0.05$). Values represent mean ± SEM. *Statistically significant difference between IGF-2/1 Tg and wild-type mice. #Statistically significant difference between IGF-2/1 Tg or wild-type mice and younger mice (1–6 months).

Results

IGF-I Peptide Concentration

To determine the specificity of Tg expression, IGF-I concentration was measured in various regions of the CNS, serum, skeletal muscle and other peripheral tissues. Figure 1A-C shows IGF-I concentration in spinal cord, brain and cerebellum. In these three CNS areas, it was significantly higher in IGF-2/1 Tg than in control wild-type mice at all ages (1, 6, 12, 18, 24 months; $n = 5$ or 6 mice; $P < 0.01$), and these values for any of the three CNS regions are similar to those noted previously for cerebellum in IGF-2/1 Tg and wild-type mice (Ye et al., 1996).

Figure 1D, E shows IGF-I concentration measured in EDL and soleus muscles, respectively. Although values in these tissues were higher than in CNS, no significant differences were detected between the concentrations measured in IGF-2/1 Tg and wild-type mice. The muscle IGF-I values reported here are similar to those measured previously in wild-type hindlimb muscles (Coleman et al., 1995; Renganathan et al., 1998). Serum IGF-I concentration values (Fig. 1F) are also similar to those reported by other labs (Coleman et al., 1995; Lang et al., 2004; Sonntag, Ramsey & Carter, 2005). These results indicate that Tg overexpression of IGF-I in CNS does not result in elevated concentrations in either muscle or serum.

To further investigate the specificity of Tg expression in the CNS, we measured IGF-I concentration in liver and kidney from 6-month-old mice. The values for IGF-2/1 Tg and wild-type mice were 195 ± 14 ($n = 5$) and 187 ± 16 ($n = 6$) pg/µg of tissue protein, respectively ($P > 0.05$). IGF-I concentration in kidney was 5.6 ± 0.6 ($n = 5$) and 4.9 ± 1.1 ($n = 5$) ng/ml for IGF-2/1 Tg and wild-type mice, respectively ($P > 0.05$). These data in liver and kidney are similar to those reported previously in wild-type rats (Fervenza et al., 1999; Li et al., 2004).

Mice and Muscle Weight

Overexpression of IGF-I in CNS did not influence mouse weight. Figure 2 compares mouse weight for the four experimental groups: young, old, IGF-2/1 Tg and wild-type. Regardless of genotype, no statistically significant difference in body weight was observed between young and old mice or when gender was considered ($P > 0.05$, $n = 15$–18 mice/group).

EDL muscle weight was significantly decreased with aging in wild-type, but not IGF-2/1 Tg, mice ($P > 0.05$, $n = 13$–15 muscles/group); young Tg mice exhibit a lower but not significantly different

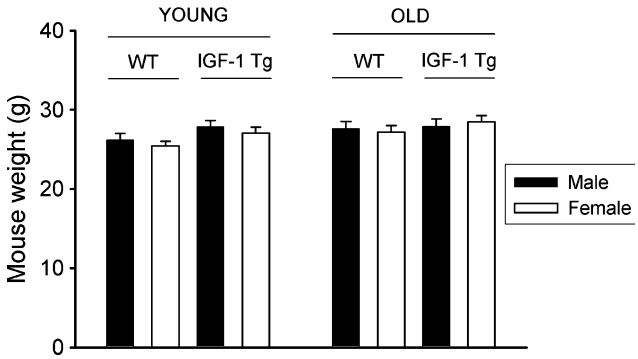

Fig. 2. Overexpression of IGF-I in the CNS does not influence mouse weight. Regardless of the genotype, body weights in young and old IGF-2/1 Tg and wild-type mice were not significantly difference. Body weights also were not significantly different between male and female mice ($P > 0.05$, $n = 15$–18 mice/group).

weight than wild-type mice. Soleus muscles from young wild-type mice are significantly different from those from young IGF-2/1 Tg mice, and muscles from old wild-type mice are significantly different from young wild-type mice (Fig. 3).

Neuromuscular Strength and Muscle-Specific Force

The hanging test is considered an assessment of neuromuscular strength (Ogura et al., 2001) because it does not require more complex skills or sophisticated motor coordination. Both scores and times were measured in the present study for six mice per group, or a total of 36 mice. Figure 4A shows the best retention time measured in wild-type mice younger than 10 (youngest was 4 months), between 10 and 18 and older than 18 (19–25) months. IGF-2/1 Tg mice older than 18 months differed significantly ($P < 0.01$) from old wild-type mice and mice younger than 10 or between 10 and 18 months ($P < 0.01$). Figure 4B shows the average retention time for the same age and genetic groups. Differences among groups were more pronounced when hanging time was computed this way. Old mice in both genetic groups exhibited a marked decline in average retention time. Additionally, IGF-2/1 Tg mice aged 10–18 months exhibited significant differences from those younger than 10 months ($P < 0.05$). The best score recorded in wild-type mice and IGF-2/1 Tg mice (Fig. 4D) exhibited a marked decline with age. Scores for middle-aged and old mice were significantly lower than for young mice ($P < 0.01$). Differences among groups were also computed as an average score (Fig. 4E). Differences between old wild-type or IGF-2/1 Tg and younger mice differed significantly ($P < 0.01$). A significant difference was also observed between middle-aged and young IGF-2/1 Tg mice ($P < 0.01$). In summary, both retention times and scores revealed a deficit in strength with aging, regardless of genotype. We recorded grip strength as a complementary test for fore- and hindlimb strength

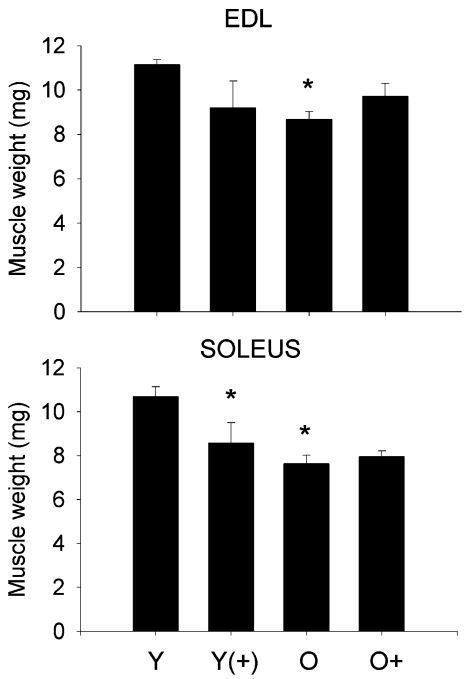

Fig. 3. EDL and soleus muscle weight declines with aging. EDL and soleus muscle weight was influenced by IGF-I overexpression in the CNS ($n = 13$–15 muscles/group). EDL and soleus muscles from aging wild-type mice are significantly different from those from young wild-type and IGF-2/1 Tg mice, while EDL and soleus muscles from old IGF-2/1 Tg did not differ significantly from those from young Tg mice. *Statistically significant difference between young (Y) and old (O) wild-type or young ($Y+$) and old ($O+$) IGF-2/1 Tg mice.

(Fig. 4). Age-dependent decline in limb strength was apparent in wild-type and IGF-2/1 Tg mice to a similar extent in both average and best performance values. These results support the conclusion that the age-dependent impairment found in retention time can be attributed to a loss in limb muscle strength that is not prevented by Tg overexpression of IGF-I in the CNS. The data on mouse retention time and limb strength are consistent with previous

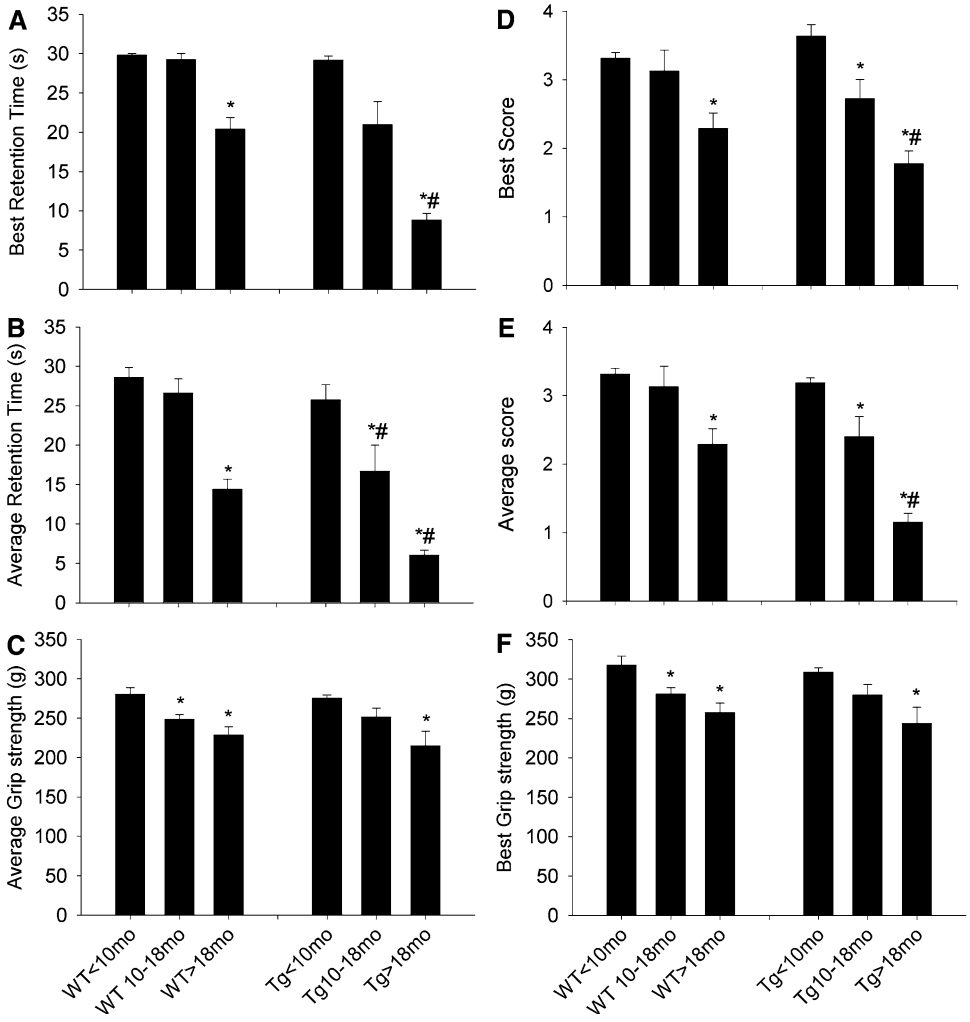

Fig. 4. Best and average retention time, score and grip strength in wild-type and IGF-2/1 Tg mice. *Significant difference compared to the younger-than-10 months group within mice of the same genotype. #Differences between age-matched wild-type and IGF-2/1 Tg mice.

publications from our (Gonzalez et al., 2000, 2003) and other (Brooks & Faulkner, 1988) laboratories on the age-dependent decrease in muscle absolute and specific force. The larger decrease in old Tg than in old wild-type mice is surprising, based on the previously reported beneficial effect of IGF-I on muscle function (*see below*). To determine whether this difference results from a decline in muscle absolute and/or specific force, EDL and soleus muscles from old mice were tested *in vitro*. A frequency/tension curve was constructed from records of the force generated in response to stimulation at increasing frequencies (González et al., 2003). Most of the muscles reached maximal tension at either 75 or 100 Hz. Figure 5A shows absolute force recorded in old wild-type (n = 13) and IGF-2/1 Tg (n = 14) EDL muscles and old wild-type (n = 14) and IGF-2/1 Tg (n = 11) soleus muscles. Absolute force in both EDL and soleus muscles declined significantly in Tg compared to wild-type mice. Figure 5B shows specific force recordings in EDL from old wild-type (n = 14) and IGF-2/1 Tg (n = 11) mice and soleus from old wild-type (n = 14) and IGF-2/1 Tg (n = 11) mice.

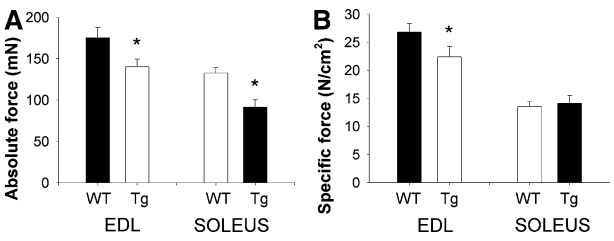

Fig. 5. Absolute and specific force in EDL and soleus muscles. (*A*) Absolute force recorded in old wild-type and IGF-2/1 Tg EDL and soleus muscles. (*B*) Specific force in EDL and soleus muscles from old wild-type and IGF-2/1 Tg mice. *Statistically significant difference between muscles from wild-type and Tg mice.

Specific force, measured as tetanic force normalized to CSA, showed a significant decline in EDL but not in soleus muscle, which indicates that loss in absolute and specific force in fast-twitch muscles accounts for the decline in muscle strength in Tg compared with wild-type mice. The specific tetanic force recorded here was similar to that reported for EDL and quadriceps muscle (Fitts et al., 1984; Eddinger,

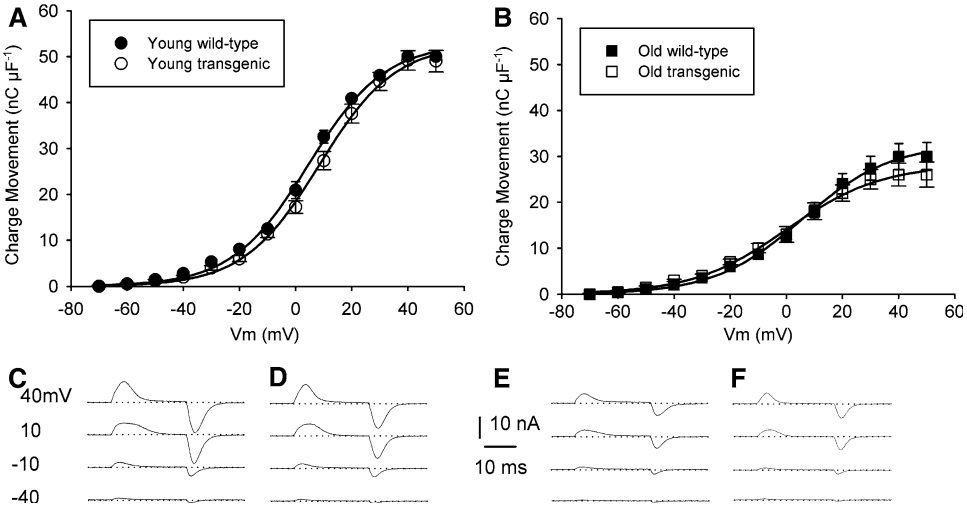

Fig. 6. Charge movement in FDB fibers from young and old mice. The charge movement/membrane voltage relationship for fibers from (*A*) young and (*B*) old wild-type and IGF-2/1 Tg mice. Data are expressed as mean ± SEM. *Continuous lines* correspond to best fitting to the data, using equation 1 (*see* Table 1). Charge movement traces (−40 to 40 m*V*) for young wild-type (*C*), young IGF-2/1 Tg (*D*), old wild-type (*E*) and old IGF-2/1 Tg (*F*) mice. *Dotted lines* indicate baseline.

Table 1. Best fitting parameters describing the voltage dependence of charge movement and intracellular Ca^{2+} concentration recorded in mouse FDB muscle fibers

	Charge movement ($nC \cdot \mu F^{-1}$)			
	Young (n = 18)	Young Tg (n = 17)	Old (n = 21)	Old Tg (n = 20)
Q_{max}	53 ± 3.1	52 ± 4.2	33 ± 2.8*	31 ± 3.2*
$V_{1/2}$	4.6 ± 0.32	6.4 ± 0.92	5.8 ± 0.67	5.3 ± 0.43
K	13.7 ± 1.1	13.6 ± 1.8	16 ± 2.3	15 ± 2.3
	Intracellular $[Ca^{2+}]$ (µM)			
	Young (n = 18)	Young Tg (n = 16)	Old (n = 18)	Old Tg (n = 18)
$[Ca^{2+}]_{max}$	1.8 ± 0.15	1.7 ± 0.24	1.1 ± 0.32*	0.9 ± 0.27*
$V_{1/2}$	8 ± 1.1	9.4 ± 1.2	8.5 ± 1.2	9.2 ± 1.4
K	8.3 ± 1.5	7 ± 0.83	6.8 ± 0.87	7.1 ± 2.1

Values are mean ± SEM with the number of fibers studied (n). *Statistically significant difference ($P < 0.05$).

Cassens & Moss, 1986) but lower than that for EDL and soleus in other publications (Brooks & Faulkner, 1988; Barton-Davis et al., 1998).

Charge Movement in Skeletal Muscle Fibers from Young and Old Wild-Type and IGF-2/1 Tg Mice

Figure 6 analyzes the voltage dependence of the charge for young and old wild-type and IGF-2/1 Tg mice. A group of charge movement traces were recorded at −40, −10, 10 and 40 m*V* in muscle fibers from young adult wild-type, IGF-2/1 Tg, old wild-type and old IGF-2/1 Tg mice. Clearly, charge movement recorded in fibers from old wild-type mice was significantly lower than that for young mice of either group. The charge moved by fibers from old IGF-2/1 Tg mice was lower than that recorded in young mice but did not differ from that recorded in old wild-type mice. Data points were fitted to a Boltzmann equation, as described in Methods. The best fitting parameters for Q_{max}, $V_{1/2Q}$ and K recorded in muscle fibers from young adult and old mice are included in Table 1. Maximum charge, but not $V_{1/2}$ or K, was significantly lower in old compared to young mice in both genetic groups. Based on these results, we conclude that the pronounced age-related decline in maximum charge movement is not prevented by sustained overexpression of IGF-I in the CNS. Differences between old wild-type and old IGF-2/1 Tg mice were not significant. These results indicate that sustained Tg overexpression of IGF-I in the CNS does not prevent the reported decrease in charge movement with aging.

Intracellular Ca^{2+} Recording

Figure 7 shows the voltage dependence of the peak Ca^{2+} transient recorded in muscle fibers from young-adult and old mice of both genetic groups from –50 to 50 m*V*. The data points were fitted to equation 1, and the best fitting parameters are included in Table 1. No significant differences in maximum Ca^{2+} concentration, Ca^{2+} transient half-activation potential ($V_{1/2}$) and steepness of the

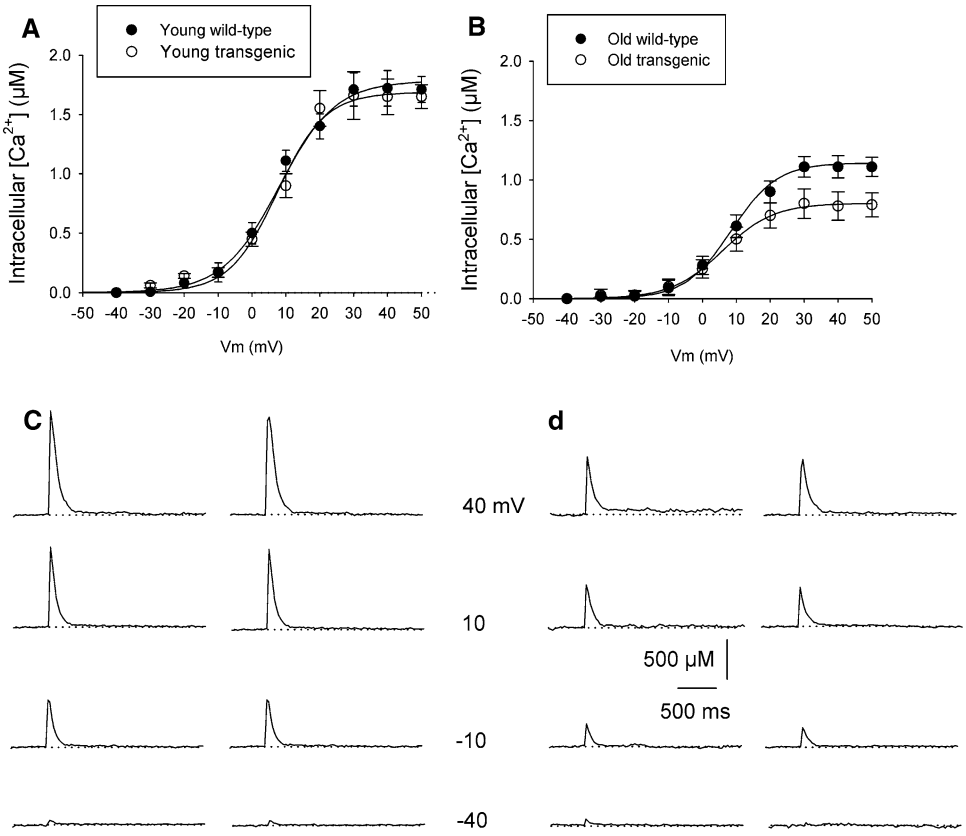

Fig. 7. Peak intracellular Ca^{2+} in FDB fibers from young and old wild-type and IGF-2/1 Tg mice. Intracellular Ca^{2+} membrane voltage relationship for fibers from (*A*) and (*B*) old wild-type and IGF-2/1 Tg mice. Data points are expressed as mean ± SEM. *Continuous lines* correspond to best fitting to the data, using equation 1 (*see* Table 1). Intracellular Ca^{2+} traces (−40 to 40 m*V*) for young wild-type and young IGF-2/1 Tg (*C*) and old wild-type and old IGF-2/1 Tg (*D*) mice. *Dotted lines* indicate the baseline.

curves between muscle fibers from young mice of both groups were found. However, the peak Ca^{2+} concentration in fibers from old mice was significantly reduced compared to fibers from young mice. Additionally, fibers from old IGF-2/1 Tg mice showed lower but not significantly different peak intracellular Ca^{2+} than fibers from old wild-type mice but no significant changes in the $V_{1/2Q}$ and steepness of the curve (Table 1). In summary, sustained overexpression of IGF-I in the CNS does not prevent the age-dependent decrease in intracellular Ca^{2+} concentration.

Figure 7C and D shows representative traces of intracellular Ca^{2+} transients recorded in fibers from young adult wild-type and IGF-2/1 Tg and from old wild-type and old IGF-2/1 Tg mice, respectively, at −40, −10, 10 and 40 m*V*. The peak intracellular Ca^{2+} recorded in fiber from the old mice was significantly smaller than that recorded in fibers from young mice, either wild-type or IGF-2/1 Tg. It is also evident that sustained overexpression of IGF-I in the CNS did not prevent the age-related decline in peak intracellular Ca^{2+} concentration.

Changes in Muscle Fiber-Type Composition with Age and Tg Overexpression of IGF-I in the CNS

SDS-PAGE analysis of the fiber-type composition of mouse EDL and soleus muscles shows four MHC isoforms: I, IIa, IIb and IIx. The predominant isoform in EDL muscle was IIb, followed by IIx, as shown in Figure 8A and B, while in soleus muscle, the IIa and I isoforms predominated (Fig. 8C, D). Figure 8A illustrates the MHC composition of representative muscles from young and old wild-type

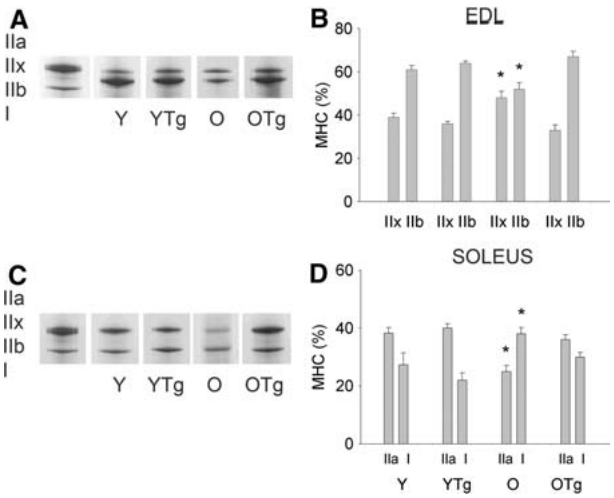

Fig. 8. Changes in muscle fiber-type composition with age and Tg overexpression of IGF-I in the CNS. SDS-PAGE analysis of the fiber-type composition of the mouse EDL (*A, B*) and soleus (*C, D*) muscles shows four MHC isoforms: I, IIa, IIb and IIx. MHC composition was expressed as a percent of the sum of all isoforms for individual muscles. *Statistically significant differences.

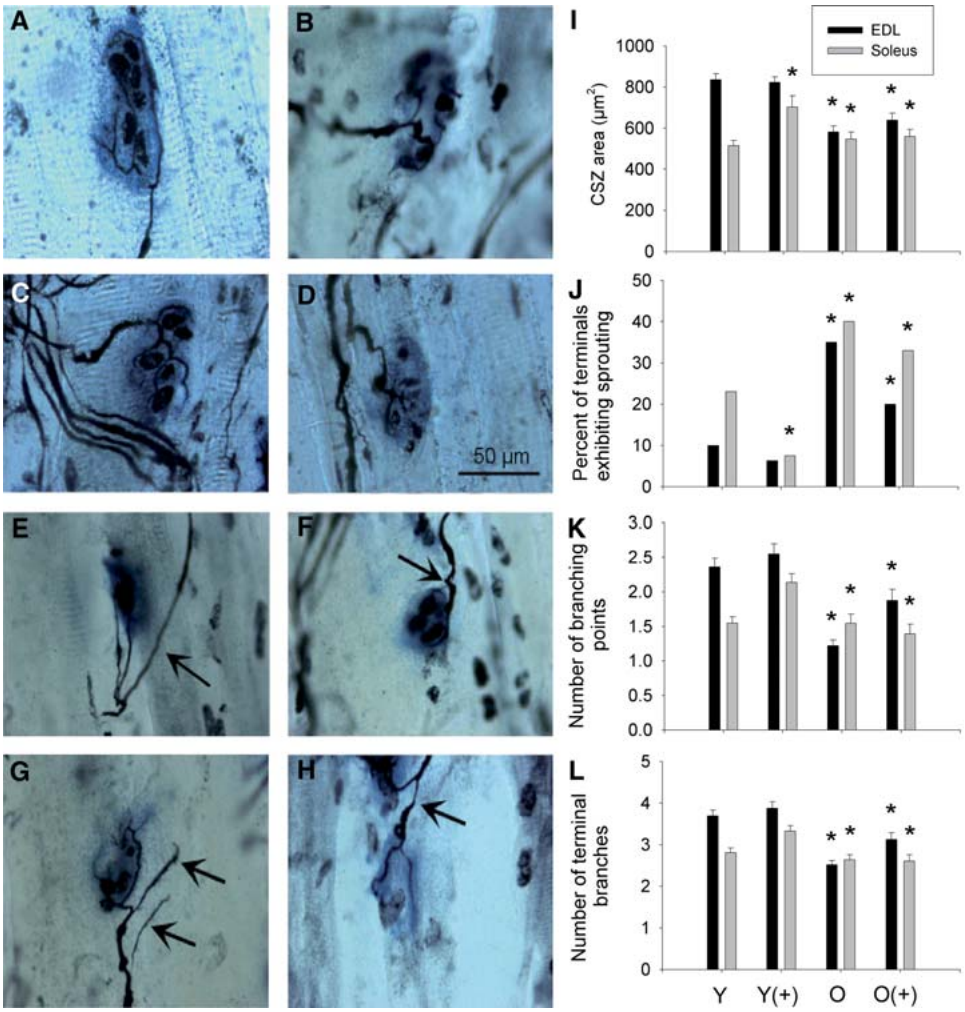

Fig. 9. Analysis of NMJ preterminals. Silver-cholinesterase staining of the axonal terminal (*dark*) and cholinesterase area (*blue*) are represented for EDL (*A*) and soleus (*B*) muscles from young wild-type and for EDL (*C*) and soleus (*D*) muscles from IGF-2/1 Tg mice. Muscles from old mice are represented for EDL (*E*) and soleus (*F*) from young wild-type mice and for EDL (*G*) and soleus (*H*) muscles from IGF-2/1 Tg mice. *Arrows* indicate sprouting. NMJ preterminal CSZ area (*I*), percent of axonal terminals exhibiting sprouting (*J*), number of axonal branching points (*K*) and number of axonal terminal branches (*L*) from young and old wild-type and IGF-2/1 Tg mice. *Significant differences compared with young wild-type or Tg mice.

and IGF-2/1 Tg mice. Figure 8B shows the MHC composition expressed as a percent of the sum of all isoforms for individual muscles. The composition of EDL muscles from young wild-type and IGF-2/1 Tg mice did not differ significantly ($P > 0.05$), whereas an increase in IIx and a decrease in IIb fibers were recorded in old wild-type mice ($P < 0.05$). Tg overexpression of IGF-I in the CNS prevented the age-dependent decrease in IIb and the increase in IIx fibers as the MHC composition of EDL muscles from the IGF-2/1 Tg mice did not differ significantly from that recorded in young wild-type or IGF-2/1 Tg mice.

Figure 8C illustrates the MHC composition of representative soleus muscles from young and old wild-type and IGF-2/1 Tg mice. Figure 8D shows that the composition of soleus muscles from young wild-type and IGF-2/1 Tg mice did not differ significantly ($P > 0.05$), while an increase in type I and a decrease in IIa fibers were recorded in old wild-type mice ($P < 0.05$). Tg overexpression of IGF-I in the CNS prevented the age-dependent decrease in IIa and increase in type I fibers. As with EDL, the MHC composition of soleus muscles from IGF-2/1 Tg mice did not differ significantly from that recorded in young wild-type or IGF-2/1 Tg mice.

Neuromuscular Junction in Aging and IGF-2/1 Tg Mice

A range of 49–64 end plates was measured from three or four muscles, each belonging to different young and old wild-type and IGF-2/1 Tg mice. Figure 9A-H illustrates the neuromuscular junction (NMJ) stained using the silver-cholinesterase method. EDL muscle from young wild-type mice shows the complexity of the nerve terminal, characterized by a number of branching points and terminal branches and absence of nerve sprouting. A smaller and simpler nerve arborization at the cholinesterase-stained zone (CSZ) was found in soleus from young wild-type mice. The complexity of the nerve terminal is maintained in EDL and soleus muscles from IGF-2/1 Tg mice. A smaller CSZ together with a simpler nerve terminal and increased nerve sprouting are apparent in EDL

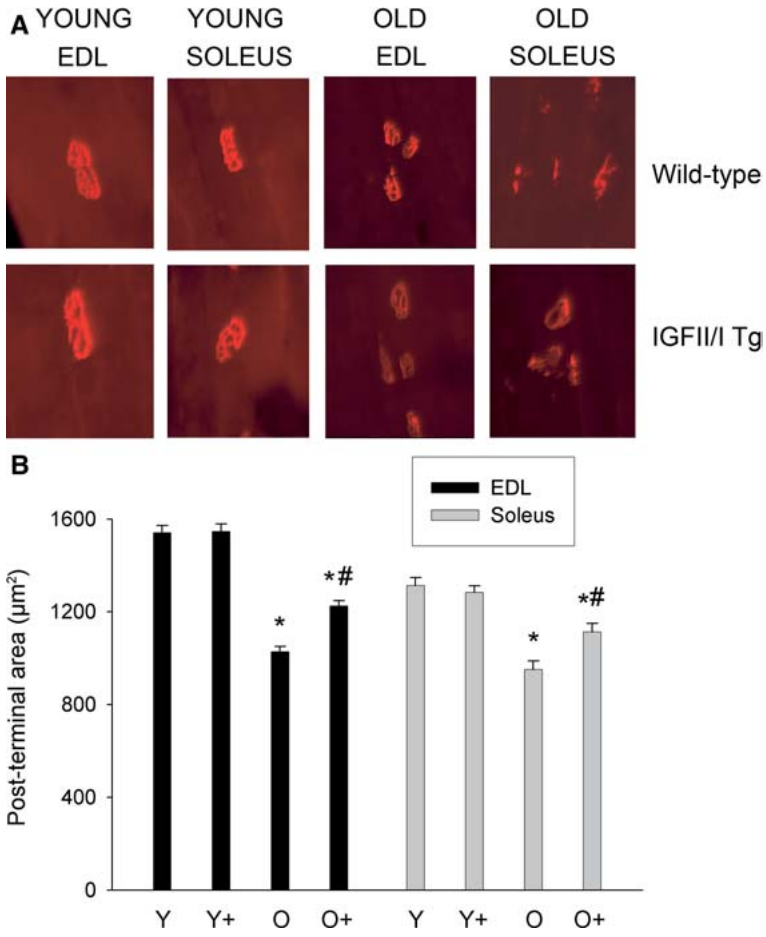

Fig. 10. Analysis of NMJ postterminals. (*A*) Postsynaptic acetylcholine receptors staining with rhodamine-conjugated α-bungarotoxin in muscle from young and old wild-type and IGF-2/1 Tg mice. (*B*) Measurements of the postterminal area delimited by fluorescent α-bungarotoxin showed a marked decrease in old wild-type mice compared to young wild-type and IGF-2/1 Tg mice ($^{*}P < 0.05$). The postterminal area was larger in IGF-2/1 Tg than in wild-type old mice for both EDL and soleus muscles ($^{\#}P < 0.05$).

and soleus muscles from old wild-type mice. A similar CSZ, increased sprouting and diminished nerve terminal complexity are obvious in EDL and soleus muscles from IGF-2/1 Tg mice.

The following four parameters were quantified for EDL and soleus muscles: end-plate area as outlined by the CSZ, percent of nerve terminals exhibiting sprouting outside the CSZ, number of nerve terminal branch points within the CSZ and percent of CSZ exhibiting nerve terminal branching (Fig. 9I-L). EDL muscles from young wild-type and IGF-2/1 Tg mice exhibit larger CSZs and more nerve branching points and terminal branches than soleus, but the percentage of terminals exhibiting nerve sprouting is larger in soleus than EDL muscles from wild-type mice, while this difference is not obvious in young IGF-2/1 Tg mice. Another interesting observation is the CSZ increase in soleus from young IGF-2/1 Tg compared to wild-type mice. EDL and soleus muscles from old wild-type mice exhibit similar CSZs, a significant increase in the percent of terminals exhibiting sprouting and simplification of nerve terminals within the CSZ characterized by fewer nerve branching points and terminal branches. Overall, CNS IGF-2/1 Tg overexpression did not modify the CSZ in EDL and soleus muscles. For both, the percentage of terminals exhibiting sprouting is higher in young wild-type mice. Similarly, a trend toward more complex nerve terminals within the CSZ is apparent; however, young mice differ significantly for both EDL and soleus muscles.

Analysis of the NMJ Postterminal

A total of 74–100 NMJs were analyzed from at least three muscles from different mice for each group (young and old wild-type and IGF-2/1 Tg). Figure 10A shows simplification, shrinkage and fragmentation of the postterminal in EDL and soleus muscles from old compared to young mice. No obvious difference in postterminal size and complexity was found between young wild-type and young Tg mice; however, old IGF-2/1 Tg exhibited larger values than old wild-type, although lower than values for younger wild-type and IGF-2/1 Tg mice. Measurements of the postterminal area delimited by fluorescent α-bungarotoxin showed a marked decrease in old wild-type mice compared to young wild-type and IGF-2/1 Tg mice ($P < 0.05$) (Fig. 10B). The postterminal area was larger in IGF-2/1 Tg than in wild-type old mice. This difference was statistically significant ($P < 0.05$).

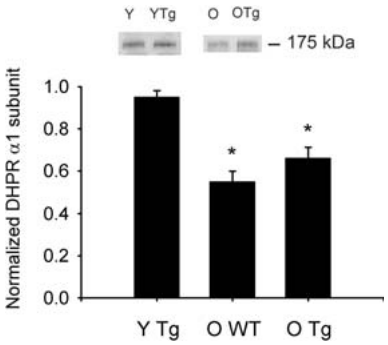

Fig. 11. Immunoblot detection of DHPR α_1-subunit. The signal at 175 kDa for young and old wild-type and IGF-2/1 Tg mice was normalized to that recorded for young wild-type mice (*top*). Values represented in the bar graph correspond to mean ± SEM. *Statistically significant differences.

DHPR α_1-Subunit Expression

We measured expression of the DHPR α_1-subunit in young and old wild-type and IGF-2/1 Tg mice by immunoblots (Fig. 11). The signal at 175 kDa for each group was normalized to that recorded for young wild-type mice (Fig. 11, top). Values represented in the bar graph correspond to mean and SEM of at least four measurements per group. The average of the expression in young IGF-2/1 Tg mice did not differ significantly from that in young wild-type mice, whereas a significant decrease was detected in old wild-type and IGF-2/1 Tg mice ($P < 0.01$). Although expression of the DHPR α_1-subunit was higher in muscles from old IGF-2/1 Tg compared to old wild-type mice, the signal was significantly lower than in muscles from young mice ($P < 0.01$).

IGF-I Expression in Lumbar Spinal Cord

To determine whether IGF-I expression is confined to the lateral motor columns, where the motor neurons that innervate hindlimbs are located, or is more diffuse, we analyzed cryosections of the lumbar enlargement of the spinal cord with an antibody specific to IGF-I. Figure 12A shows IGF-I immunofluorescence in young wild-type mice. The signal is strongly enhanced in the spinal cord from young Tg mice (Fig. 12B). Arrows indicate both lateral motor columns intensively immunoreacting with IGF-I antibody. IGF-I immunostaining can be appreciated at higher magnification in the lateral motor column area (Fig. 12D, F). In addition to the localization of IGF-I to this area, a diffuse pattern of its expression is observed in the ventral, intermediate, dorsal and peripheral to the central canal areas. These data, based on 18–22 sections from three or four mice per group, suggest IGF-I expression in the spinal cord is not exclusively in motor neurons. We observed a lower fluorescence signal in old wild-type mice (Fig. 12C) and higher expression in spinal cords from old IGF-2/1 Tg mice, similar to that recorded in young IGF-2/1 Tg mice (Fig. 12E).

Discussion

We tested the hypothesis that exclusive and sustained overexpression of IGF-I in the CNS improves muscle strength and overall physical performance by preventing or delaying age-dependent alterations in muscle innervation, NMJ postterminal architecture and excitation-contraction coupling. We found that (1) the IGF-I transgene is expressed extensively across the spinal cord gray matter in addition to the lateral motor column, (2) Tg IGF-I expression in the CNS does not modify mouse weight regardless of the decline in muscle weight with aging and (3) muscle performance showed significantly decreased retention time and limb strength in Tg compared to wild-type mice, which is consistent with decreased absolute and specific force measured in the EDL muscle *in vitro*. These results are consistent with decreased charge movement and peak intracellular Ca^{2+} mobilization in individual muscle fibers from old IGF-2/1 Tg compared with young wild-type mice. Lack of improvement in charge movement and intracellular Ca^{2+} mobilization in old Tg compared with old wild-type or young mice is associated with decreased DHPR α_1-subunit expression in muscles from old IGF-2/1 Tg compared with young mice. Tg IGF-I overexpression in the CNS prevented the switches in muscle fiber-type composition, which are associated with improvement in muscle innervation, as revealed by analysis of the NMJ pre- and postterminal structure in old IGF-2/1 Tg mice. The results reported here do not confirm our hypothesis and raise questions about the timing and/or location of IGF-I overexpression in the CNS needed to prevent or to ameliorate age-dependent alterations to the structure and function of skeletal muscle.

Muscle Strength and Excitation-Contraction Coupling

The finding that Tg overexpression of IGF-I in the CNS did not improve retention time/score, muscle strength and absolute and specific force *in vitro* in old mice was surprising based on previous communications about the beneficial effect of IGF-I overexpressed in muscle (Barton-Davis et al., 1998; Renganathan et al., 1998; Musaro et al., 2001) or retrograde-transported into motor neurons (Payne et al., 2006) on muscle and neuromuscular structure and function (González et al., 2003; Messi & Delbono, 2003), charge movement and peak intracellular Ca^{2+} mobilization *in vitro* (Wang et al., 2002). Additionally, the lack of improvement in charge movement

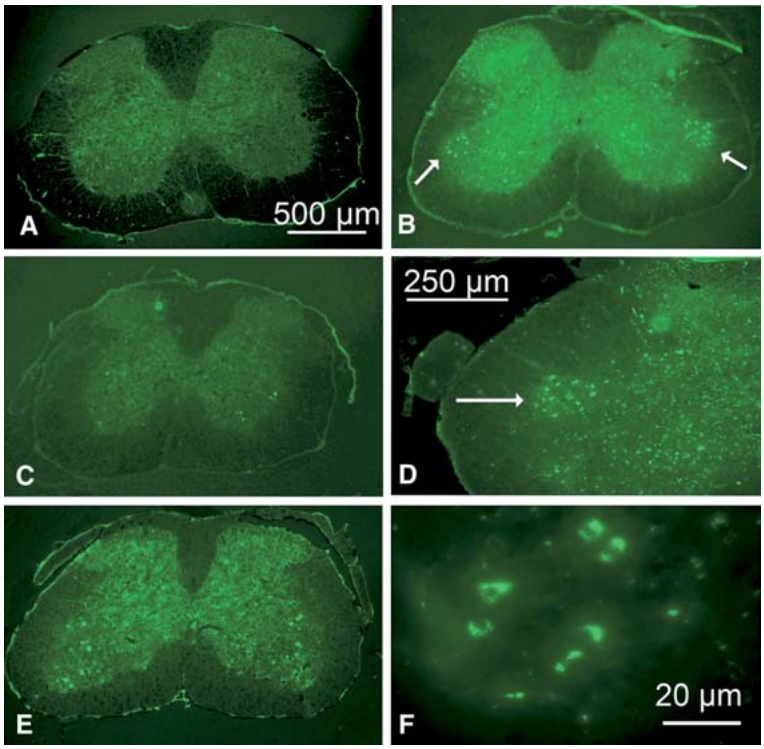

Fig. 12. IGF-I immunofluorescence in lumbar spinal cord. (*A*) Young wild-type. (*B*) Young IGF-2/1 Tg. (*C*) Old wild-type. (*D*) Enlargement of the lumbar spinal cord section from an IGF-2/1 Tg mouse to visualize the lateral motor column (LMC). (*E*) Old IGF-2/1 Tg. (*F*) Detail of motor neurons in the LMC from an IGF-2/1 Tg mouse. *Arrows* indicate the location of the LMC in the spinal cord section.

and intracellular Ca^{2+} mobilization is associated with decreased expression of DHPR α_1-subunit in muscles from old IGF-2/1 Tg mice. We have demonstrated that muscle IGF-I enhances DHPR α_1-subunit transcriptional activity by acting on the cAMP-response element-binding protein element of the promoter region (Zheng et al., 2002), an effect mediated by Ca^{2+}-calmodulin kinase and calcineurin (Zheng et al., 2004). Whether this phenomenon operates when IGF-I is overexpressed in spinal cord motor neurons is not known. Also, whether rescue of single muscle fiber-specific force from old mice by retrograde transport of IGF-I from muscle to motor neuron is mediated by enhanced expression of DHPR α_1-subunit is not known. However, the effects of motor neuron-targeted IGF-I on muscle fiber-specific force, but not on diameter and absolute force, indicate that IGF-I improves muscle function by preventing or reversing excitation-contraction uncoupling and not by acting on muscle mass or contractile proteins (Payne et al., 2006).

IGF-I/tetanus toxin fragment C-mediated preservation of muscle-specific force indicates that indemnity of muscle innervation is necessary and sufficient to sustain this muscle function across ages (Payne et al., 2006). The main difference between the fusion protein model and the CNS IGF-I Tg used here is the former's retrograde transport of IGF-I, which ensures a predominant motor neuron location, while in the latter the growth factor expression pattern is diffuse. This difference may suggest that IGF-I expression in spinal cord cells other than motor neurons counterbalances the beneficial effect of motor neuron IGF-I on excitation-contraction coupling, supported by the lack of a significant increase in DHPR α_1 expression, charge movement and intracellular Ca^{2+} mobilization in IGF-2/1 Tg mice compared to wild-type old mice. The specific population of spinal cord cells (neuron, glia or interneuron) potentially counteracting the beneficial expression of IGF-I in motor neurons is unknown.

It also is possible that the incomplete restoration of muscle innervation and postterminal structure in old IGF-2/1 Tg mice is due to insufficiently high IGF-I overexpression. The modest increases in spinal cord IGF-I concentration in IGF-2/1 argue for this possibility. Nonetheless, such increases in CNS IGF-I concentration result in marked phenotypic changes in the CNS, e.g., doubling of cerebellar size (Ye et al., 1996; D'Ercole, Ye & O'Kusky, 2002). In contrast, the S1S2 muscle IGF-I Tg model exhibits a >40-fold increase in local IGF-I concentration (Coleman et al., 1995) compared to a 1.5- to 2.0-fold increase in the IGF-2/1 mouse CNS. Our findings, however, indicate that the modest degree of IGF-I overexpression in IGF-2/1 Tg is sufficient to effect biological change. We found that CNS overexpression of IGF-I prevents switches in muscle fiber-type composition. Muscle fiber phenotype is determined by interactions with subpopulations of ventral spinal cord motor neurons that activate contraction at different rates, ranging from 10 (slow) to 100 (fast fatigue-resistant)

or 150 Hz (fast fatigue-sensitive) fibers (Buller, Eccles & Eccles, 1960a, 1960b; Greensmith & Vrbova, 1996). Age-dependent preservation of motor neuron firing rate and myelination (Ye et al., 2002; D'Ercole et al., 2002) may help to maintain muscle phenotype throughout the mouse life span.

We confirm that aging skeletal muscle exhibits alterations in fiber innervation. Several groups have reported skeletal muscle denervation and reinnervation and motor unit remodeling or loss in aging rodents or humans (Hashizume, Kanda & Burke, 1988; Kanda & Hashizume, 1989; Zhang et al., 1996; *for review, see* Delbono, 2003). Motor unit remodeling leads to changes in fiber-type composition (Pette & Staron, 2001). We have reported that old muscles from IGF-I Tg (S1S2) mice do not exhibit major alterations in the nerve terminal and structure of the NMJ postterminal, which is associated with preservation of muscle fiber phenotype (Messi & Delbono, 2003). Improvements in muscle innervation and postterminal structure along with conservation of muscle fiber phenotype in aging IGF-2/1 Tg mice, reported in this work, are therefore not surprising. Although both pre- and postterminal NMJs in old IGF-2/1 Tg mice exhibit an intermediate pattern between young (wild-type or Tg) and old wild-type mice, analysis of muscle fiber-type composition indicates that these changes are sufficient to preserve the young fiber phenotype profile.

IGF-I Tg Model

To our knowledge, this study is the first to examine muscle function and the structure/function of muscle innervation in mice that overexpress IGF-I exclusively in the CNS. IGF-2/1 Tg mice (Ye et al., 1996) overexpress IGF-I exclusively in the CNS without any evidence of direct systemic influence in adult and aging animals, due to the lack of systemic leakage or expression in peripheral tissues, as demonstrated by the absence of the transgene in various organs, including fast- and slow-twitch muscles in young, middle-aged and old mice. The reason for the reduced serum IGF-I concentration in IGF-2/1 Tg compared with wild-type mice is not known, but we speculate that expression of hIGF-I transgene in the brain inhibits the expression and release of growth hormone, which is a key regulator for liver IGF-I expression, a major source for serum IGF-I.

This model does not predict more spinal cord motor neurons in IGF-2/1 Tg compared to wild-type mice, based on the postnatal expression of the transgene, at which time programmed motor neuron death has already taken place (Oppenheim, 1996; Ye et al., 1996), and in contrast to the increased number of neurons and synapses in other areas of the CNS, such as the hippocampus dentate gyrus (O'Kusky, Ye & D'Ercole, 2000). In normal mice, neurogenesis in this area occurs predominantly between embryonic day 14 and postnatal day 20 (Stanfield & Cowan, 1979). Similarly, IGF-2/1 Tg mice exhibit increased proliferation of cerebellum granule cell progenitors (Ye et al., 1996). These findings support the concept that the IGF-I transgene not only expresses but also exhibits biological activity. That it exerts biological activity in the spinal cord motor neurons is reflected in the prevention of age-dependent muscle fiber-type switching.

An interesting aspect of our study is the finding that Tg expression of IGF-I is not exclusive to the lateral motor column motor neurons. Positive immunofluorescence was detected across the spinal cord section in neuronal and probably glial cells throughout the Rexed lamina, including anterior, dorsal horns and pericentral canal. Whether overexpression of IGF-I in cells other than spinal cord motor neurons offsets the beneficial effects described for the predominantly motor neuron-expressing model (Payne et al., 2006) is not yet known. A common factor for Tg mice overexpressing IGF-I in the CNS is overgrowth of the brain (Popken et al., 2004). This phenomenon does not result in motor alterations at a young age, as demonstrated by the absence of motor impairment in the present study; however, whether survival of a number of neurons committed to die in the postnatal (IGF-2/1 mouse model) or the embryonic and postnatal (Popken et al., 2004) period has deleterious consequences for aging mammals is not known.

The present study was supported by grants from the National Institutes of Health-National Institute on Aging (AG13934 and AG15820) and the Muscular Dystrophy Association (to O. D.), the National Institute for Human Development (NIHD) (HD008299, to J. A. D.) and the Wake Forest University Claude D. Pepper Older Americans Independence Center (P30-AG21332). We thank Ms. Julie Edelson for editing the manuscript.

References

Barton-Davis, E.R., Shoturma, D.I., Musaro, A., Rosenthal, N., Sweeney, H.L. 1998. Viral mediated expression of insulin-like growth factor I blocks the aging-related loss of skeletal muslce function. *Proc. Natl. Acad. Sci. USA* **95:**15603–15607

Brooks, S.V., Faulkner, J.A. 1988. Contractile properties of skeletal muscles from young, adult and aged mice. *J. Physiol.* **404:**71–82

Buller, A.J., Eccles, J. C., Eccles, R.M. 1960a. Differentiation of fast and slow muscles in the cat hind limb. *J. Physiol.* **150:**399–416

Buller, A.J., Eccles, J. C., Eccles, R.M. 1960b. Interactions between motoneurones and muscles in respect of the characteristic speeds of their responses. *J. Physiol.* **150:**417–439

Caroni, P., Grandes, P. 1990. Nerve sprouting in innervated adult skeletal muscle induced by exposure to elevated levels of insulin like growth factors. *J. Cell Biol.* **110:**1307–1317

Coleman, M.E., DeMayo, F., Yin, K.C., Lee, H.M., Geske, R., Montgomery, C., Schwartz, R.J. 1995. Myogenic vector expression of insulin-like growth factor I stimulates muscle cell

differentiation and myofiber hypertrophy in transgenic mice. *J. Biol. Chem.* **270:**12109–12116

Dai, Z., Takahashi, S.I., Wyk, J.J., D'Ercole, A.J. 1992. Creation of an autocrine model of insulin-like growth factor-I action in transfected FRTL-5 cells. *Endocrinology* **130:**3175–3183

Delbono, O. 2003. Neural control of aging skeletal muscle. *Aging Cell* **2:**21–29

D'Ercole, A.J., Ye, P., O'Kusky, J.R. 2002. Mutant mouse models of insulin-like growth factor actions in the central nervous system. *Neuropeptides* **36:**209–220

Dobrowolny, G., Giacinti, C., Pelosi, L., Nicoletti, C., Winn, N., Barberi, L., Molinaro, M., Rosenthal, N., Musaro, A. 2005. Muscle expression of a local IGF-I isoform protects motor neurons in an ALS mouse model. *J. Cell Biol.* **168:**193–199

Eddinger, T.J., Cassens, R.G., Moss, R.L. 1986. Mechanical and histochemical characterization of skeletal muscles from senescent rats. *Am. J. Physiol.* **251:**C421–C430

Einsiedel, L.J., Luff, A.R. 1992. Effect of partial denervation on motor units in the ageing rat medial gastrocnemius. *J. Neurol. Sci.* **112:**178–184

Fervenza, F.C., Tsao, T., Hsu, F., Rabkin, R. 1999. Intrarenal insulin-like growth factor-1 axis after unilateral nephrectomy in rat. *J. Am. Soc. Nephrol.* **10:**43–50

Fitts, R.H., Troup, J.P., Witzmann, F.A., Holloszy, J.O. 1984. The effect of ageing and exercise on skeletal muscle function. *Mech. Ageing Dev.* **27:**161–172

Florini, J.R., Ewton, D.Z., Coolican, S.A. 1996. Growth hormone and insulin growth factor system in myogenesis. *Endocr. Rev.* **17:**481–517

Giulian, G.G., Moss, R.L., Greaser, M. 1983. Improved methodology for analysis and quantitation of proteins on one dimensional silver-stained slab gels. *Anal. Biochem.* **129:**277–287

Gonzalez, E., Messi, M.L., Delbono, O. 2000. The specific force of single intact extensor digitorum longus and soleus mouse muscle fibers declines with aging. *J. Membr. Biol.* **178:**175–183

González, E., Messi, M.L., Zheng, Z., Delbono, O. 2003. Insulin-like growth factor-1 prevents age-related decrease in specific force and intracellular Ca^{2+} in single intact muscle fibres from transgenic mice. *J. Physiol.* **552:**833–844

Greensmith, L., Vrbova, G. 1996. Motoneurone survival: A functional approach. *Trends Neurosci.* **19:**450–455

Hashizume, K., Kanda, K., Burke, R. 1988. Medial gastrocnemius motor nucleus in the rat: Age-related changes in the number and size of motoneurons. *J. Comp. Neurol.* **269:**425–430

Kadhiresan, V.A., Hassett, C.A., Faulkner, J.A. 1996. Properties of single motor units in medial gastrocnemius muscles of adult and old rats. *J. Physiol.* **493:**543–552

Kanda, K., Hashizume, K. 1989. Changes in properties of the medial gastrocnemius motor units in aging rats. *J. Neurophysiol.* **1989:**737–746

Kanje, M., Skottner, A., Sjoberg, J., Lundborg, G. 1989. Insulin-like growth factor I (IGF-I) stimulates regeneration of the rat sciatic nerve. *Brain Res.* **486:**396–398

Knudson, C.M., Chaudhari, N., Sharp, A.H., Powell, J.A., Beam, K.G., Campbell, K.P. 1989. Specific absence of the alpha 1 subunit of the dihydropyridine receptor in mice with muscular dysgenesis. *J. Biol. Chem.* **264:**1345–1348

Lang, C.H., Frost, R.A., Svanberg, E., Vary, T.C. 2004. IGF-I/IGFBP-3 ameliorates alterations in protein synthesis, eIF4E availability, and myostatin in alcohol-fed rats. *Am. J. Physiol.* **286:**E916–E926

Larsson, L., Ansved, T. 1995. Effects of ageing on the motor unit. *Prog. Neurobiol.* **45:**397–458

Leung, A.T., Imagawa, T., Campbell, K.P. 1987. Structural characterization of the 1,4-dihydropyridine receptor of the voltage-dependent Ca^{2+} channel from rabbit skeletal muscle. Evidence for two distinct high molecular weight subunits. *J. Biol. Chem.* **262:**7943–7946

Lexell, J. 1995. Human aging, muscle mass, and fiber type composition. *J. Gerontol. A Biol. Sci. Med. Sci.* **50:**11–16

Li, D., Sweeney, G., Wang, Q., Klip, A. 1999. Participation of PI3K and atypical PKC in Na^+-K^+-pump stimulation by IGF-I in VSMC. *Am. J. Physiol.* **276:**H2109–H2116

Li, J.B., Wang, C.Y., Chen, J.W., Feng, Z.Q., Ma, H.T. 2004. Expression of liver insulin-like growth factor 1 gene and its serum level in patients with diabetes. *World J. Gastroenterol.* **10:**255–259

Li, X., Oppenheim, R.W., Lei, M., Houenou, L.J. 1994. Neurotrophic agents prevent motoneuron death following sciatic nerve section in the neonatal mouse. *J. Neurobiol.* **25:**759–766

Messi, M.L., Delbono, O. 2003. Target-derived trophic effect on skeletal muscle innervation in senescent mice. *J. Neurosci.* **23:**1351–1359

Meyer, O.A., Tilson, H.A., Byrd, W.C., Riley, M.T. 1979. A method for the routine assessment of fore- and hindlimb grip strength of rats and mice. *Neurobehav. Toxicol.* **1:**233–236

Mourkioti, F., Rosenthal, N. 2005. IGF-I, inflammation and stem cells: Interactions during muscle regeneration. *Trends Immunol.* **26:**535–542

Murray, B.E., Ohlendieck, K. 1997. Cross-linking analysis of the ryanodine receptor and alpha1-dihydropyridine receptor in rabbit skeletal muscle triads. *Biochem. J.* **324:**689–696

Musaro, A., McCullagh, K.J., Paul, A., Houghton, L., Dobrowolny, G., Molinaro, M., Barton-Davis, E.R., Sweeney, H.L., Rosenthal, N. 2001. Localized IGF-I transgene expression sustains hypertrophy and regeneration in senescent skeletal muscle. *Nat. Genet.* **27:**195–200

Neff, N.T., Prevette, D.M., Houenou, L.J., Lewis, M.E., Glicksman, M.A., Yin, Q.-W., Oppenheim, R.W. 1993. Insulin-like growth factors: Putative muscle-derived trophic agents that promote motoneuron survival. *J. Neurobiol.* **24:**1578–1588

O'Kusky, J.R., Ye, P., D'Ercole, J. 2000. Insulin-Like growth factor-1 promotes neurogenesis and synaptogenesis in the hippocampal dentate gyrus during postnatal development. *J. Neurosci.* **15:**8435–8442

Ogura, H., Aruga, J., Mikoshiba, K. 2001. Behavioral abnormalities of Zic1 and Zic2 mutant mice: Implications as models for human neurological disorders. *Behav. Genet.* **31:**317–324

Oppenheim, R.W. 1996. Neurotrophic survival molecules for motoneurons: An embarrassment of riches. *Neuron* **17:**195–197

Payne A.M., Delbono O. 2004. Neurogenesis of excitation-contraction uncoupling in aging skeletal musule. Exerc Sport Sci Rev. 32:36–40

Payne, A.M., Zheng, Z., Messi, M.L., Milligan, C.E., Gonzalez, E., Delbono, O. 2006. Motor neurone targeting of IGF-I prevents specific force decline in ageing mouse muscle. *J. Physiol.* **570:**283–294

Pestronk, A., Drachman, D.B. 1978. A new stain for quantitative measurement of sprouting at neuromuscular junctions. *Muscle Nerve* **1:**70–74

Pette, D., Staron, R.S. 2001. Transitions of muscle fiber phenotypic profiles. *Histochem. Cell Biol.* **115:**359–372

Popken, G.J., Hodge, R.D., Ye, P., Zhang, J., Ng, W., O'Kusky, J.R., D'Ercole, A.J. 2004. In vivo effects of insulin-like growth factor-I (IGF-I) on prenatal and early postnatal development of the central nervous system. *Eur. J. Neurosci.* **19:**2056–2068

Rabinovsky, E.D., Gelir, E., Gelir, S., Lui, H., Kattash, M., DeMayo, F.J., Shenaq, S.M., Schwartz, R.J. 2003. Targeted expression of IGF-I transgene to skeletal muscle accelerates muscle and motor neuron regeneration. *FASEB J.* **17:**53–55

Renganathan, M., Messi, M.L., Delbono, O. 1998. Overexpression of IGF-I exclusively in skeletal muscle prevents age-related

decline in the number of dihydropyridine receptors. *J. Biol. Chem.* **273:**28845–28851

Sacco, A., Regis, D., LaBarge, M.A., Hammer, M.M., Kraft, P., Blau, H.M. 2005. IGF-I increases bone marrow contribution to adult skeletal muscle and enhances the fusion of myelomonocytic precursors. *J. Cell Biol.* **171:**483–492

Segal, S.S., Faulkner, J.A. 1985. Temperature-dependent physiological stability of rat skeletal muscle in vitro. *Am. J. Physiol.* **248:**C265–C270

Serrano, A.L., Petrie, J.L., Rivero, J.L.L., Hermanson, J.W. 1996. Myosin isoforms and muscle fiber characteristics in equine gluteus medius muscle. *Anat. Rec.* **244:**444–451

Sonntag, W.E., Ramsey, M., Carter, C.S. 2005. Growth hormone and insulin-like growth factor-1 (IGF-I) and their influence on cognitive aging. *Ageing Res. Rev.* **4:**195–212

Stanfield, B.B., Cowan, W.M. 1979. The morphology of the hippocampus and dentate gyrus in normal and reeler mice. *J. Comp. Neurol.* **185:**393–422

Su, J.L., Stimpson, S., Edwards, C., Arnold, J., Burgess, S., Lin, P. 1997. Neutralizing IGF-I monoclonal antibody with cross-species reactivity. *Hybridoma* **16:**513–518

Tsien, R.W., Pozzan, T. 1989. Measurement of cytosolic free Ca^{2+} with quin2: Practical aspects. *Methods Enzymol.* **172:**230–262

Wang, Z.-M., Messi, M.L., Delbono, O. 2000. L-type Ca^{2+} channel charge movement and intracellular Ca^{2+} in skeletal muscle fibers from aging mice. *Biophys. J.* **78:**1947–1954

Wang, Z.-M., Messi, M.L., Delbono, O. 2002. Sustained overexpression of IGF-I prevents age-dependent decrease in charge movement and intracellular calcium in mouse skeletal muscle. *Biophys. J.* **82:**1338–1344

Wang, Z.M., Messi, M.L., Delbono, O. 1999. Patch-clamp recording of charge movement, Ca^{2+} current and Ca^{2+} transients in adult skeletal muscle fibers. *Biophys. J.* **77:**2709–2716

Ye, P., Li, L., Richards, R.G., DiAugustine, R.P., D'Ercole, A.J. 2002. Myelination is altered in insulin-like growth factor-I null mutant mice. *J. Neurosci.* **22:**6041–6051

Ye, P., Xing, Y., Dai, Z., D'Ercole, J. 1996. In vivo actions of insulin-like growth factor-I (IGF-I) on cerebellum development in transgenic mice: Evidence that IGF-I increases proliferation of granule cells progenitors. *Dev. Brain Res.* **95:**44–54

Zhang, C., Goto, N., Suzuki, M., Ke, M. 1996. Age-related reductions in number and size of anterior horn cells at C6 level of the human spinal cord. *Okajimas Folia Anat. Jpn.* **73:**171–177

Zheng, Z., Wang, Z.M., Delbono, O. 2002. Insulin-like growth factor-1 increases skeletal muscle DHPR $alpha_{1S}$ transcriptional activity by acting on the cAMP-response element-binding protein element of the promoter region. *J. Biol. Chem.* **277:**50535–50542

Zheng, Z., cWang, Z.M., Delbono, O. 2004. Ca^{2+} calmodulin kinase and calcineurin mediate IGF-I-induced skeletal muscle dihydropyridine receptor $alpha_{1S}$ transcription. *J. Membr. Biol.* **197:**101–112